Flexible and Printed Electronics

Printed hybrid capacitive Kirigami sensor: enhancing flexibility and conformability for improved motion artifacts

To cite this article: Laura Morelli *et al* 2024 *Flex. Print. Electron.* **9** 045012

IOP Publishing Flex. Print. Electron. 9 (2024) 045012 https://doi.org/10.1088/2058-8585/ad9ec0

Flexible and Printed Electronics

OPEN ACCESS

RECEIVED
19 June 2024

REVISED
13 October 2024

ACCEPTED FOR PUBLICATION
10 December 2024

PUBLISHED
24 December 2024

PAPER

Printed hybrid capacitive Kirigami sensor: enhancing flexibility and conformability for improved motion artifacts

Laura Morelli[1], **Arjun Wadhwa**[2], **Sylvain Cloutier**[2], **Martin Bolduc**[3], **Ghyslain Gagnon**[2] and **Ricardo J Zednik**[1,*]

[1] Department of Mechanical Engineering, École de technologie supérieure, Montréal, QC, Canada
[2] Department of Electrical Engineering, École de technologie supérieure, Montréal, QC, Canada
[3] Department of Mechanical Engineering, Université du Québec à Trois-Rivières, Trois-Rivières QC, Canada
* Author to whom any correspondence should be addressed.

E-mail: ricardo.zednik@etsmtl.ca

Keywords: capacitive sensing, printed electronics, inkjet printing, flexible hybrid sensors, Kirigami

Abstract

Capacitive sensing of electrophysiological signals is a promising alternative to traditional contact-type sensing for long-term and ubiquitous health monitoring. Many researchers are focusing on developing flexible capacitive electrodes to improve the conformability and the quality of acquisition of this family of sensors. However, current flexible devices still present many limitations due to the negative Poisson's ratio of the materials used, which affects the dimensions and characteristics of the materials when under stress, and their incompatibility with traditional manufacturing methods and solid-state devices. We present a novel, inkjet-printed, hybrid capacitive Kirigami sensor design. This novel structure comprises different layers with different functionalities, in order to allow improved flexibility and conformability of the flexible Kirigami printed electrode, while securing its inclusion on a traditional rigid printed circuit board for a quality signal acquisition. The novel sensor design has been tested on different shapes and dimensions of sensing target and with different weights applied. Capacitive and electrical measurements were performed to obtain the main basic sensor characteristics such as coupled capacitance, acquired signal amplitude and cutoff frequency. When compared to an analog but rigid sensor, the novel designed hybrid flexible sensor showed significant improvement and enhanced uniformity of measurements, with an increase in amplitude value up to +82% for the bigger curvatures, while maintaining good electrical contact and integrity of all the layers.

1. Introduction

In recent years, the interest in non-invasive and continuous monitoring of physiological signals has triggered significant advancements in sensor technologies [1–4]. Capacitive sensing, in particular, has emerged as a promising technique for contactless biopotential monitoring, offering advantages such as high sensitivity, low power consumption, and compatibility with wearable devices [5–8]. For this application, the body surface and the electrode can be respectively considered as the two sides of a capacitor: the capacitance is established by the close vicinity of the two surfaces and no direct contact is needed. This allows the electrophysiological signal coming from the body to be acquired without the need for gels or adhesives, without specific medical preparation, and including fabric between the body and sensing electrode [9–11].

This family of sensors is a promising substitute for long-term applications and ubiquitous sensing. However, they still present some major limitations due to their contactless nature [11, 12]: motion artifacts (MAs) are significantly larger compared to gel-type contact sensors and, depending on the relative position of the body on the sensor, the effective area of the capacitive coupling can vary, decreasing the signal-to-noise ratio (SNR) and affecting the uniformity of the measurements.

Many works can be found in the literature that use different and innovative post-processing techniques to restore the acquired signal in case of bad acquisition set-ups and MAs [13–15]. However, excessive

filtering and processing can result in additional artifacts and loss of information in the signal, while also increasing the total complexity, cost, and power consumption of the final sensor [10, 12, 16]. It is thus important to put as much emphasis on the development of the electrode side of the sensor.

As the working principle of this type of sensor is based on the parallel plate capacitance relation, $C = \epsilon_0 \epsilon_r \frac{A}{d}$, where A is the surface area of the electrode that is able to establish a capacitive coupling with the body, d is the distance between the electrode and the body (which takes into account the dielectric presence) and ϵ_0,ϵ_r are the dielectric permittivity of vacuum and of the relative dielectric constant between the two electrodes. The geometrical characteristics of the sensor electrode and the coupling mechanism between the electrode and the body are of extreme importance for a good quality signal acquisition [17]: the higher the capacitance established between the electrode and the body, the higher the SNR at the input of the sensor amplifier and the lower the cutoff frequency, which is of critical importance for a lossless signal acquisition [16, 18].

Flexibility is a crucial aspect in the development of capacitive sensors as the human body is not, in general, a flat surface:

- Adapting to any body shape allows the whole surface of the sensor to establish a capacitive coupling with the body, maximizing the effective capacitance and consequently the SNR.
- Conformability also reduces the effect of MAs, such as the one resulting from the movement of the body during respiratory activity. Motion artifacts represent one of the major issues of capacitive sensing, as a direct result of the contactless nature of capacitive sensors [8, 19].
- By conforming evenly to different parts of the body, the sensing area is ideally constant, regardless of the point of application of the sensor on the body. This allows a uniform signal acquisition, especially in multi-sensor array systems, which translates into reduced active filtering in the signal post-processing phase, and thus less susceptibility to data attenuation [16].

1.1. Flexible hybrid electronics and Kirigami electronics

The recent growth in the field of printed electronics [20] has fuelled fast developments in sensors ranging from capacitance, pressure, temperature, and humidity detection [21]. Printed electronics utilize conductive, semi-conductive, or insulating inks on flexible substrates (such as plastic or paper) using methods such as screen printing, inkjet printing, gravure or flexographic printing. Piezoelectric-based inkjet printing [22, 23] has been successfully employed to rapidly prototype and fabricate devices such as RFID tags, temperature sensors, strain gauges, etc. The printing technique's benefits are attributed to its ease of design iterations, as a result of digital design file input, and ultra-low volume material consumption, generally in the range of 1–3 ml, allowing the use of small quantities for high-cost materials such as silver, copper, and gold to fabricate functional devices [24].

Many recent works have been focusing on the development of printed flexible devices, in particular employing flexible materials for the realization of the capacitive electrode [8, 16, 25–28]. However, when flexed or stretched, these materials change in dimension depending on their Poisson's ratio and, when subjected to mechanical stress, their electric and dielectric properties are affected [29, 30], impacting the uniformity and the reliability of the measurements.

Flexible hybrid electronics (FHE) represents a sought-after alternative for the development of lightweight, conformable, and stretchable systems [31–33]: by seamlessly integrating the mechanical flexibility of flexible printed substrates with the high performance of traditional rigid electronics it promises significant advancements in developing wearable sensors that offer both comfort and performance. Several different works have employed FHE to build flexible capacitive sensors for biopotential monitoring, with promising results, as displayed in table 1.

While constituting a promising compromise between whole-flexible electronics and solid-state electronics, challenges such as robust electrical connections between different materials and components, mechanical fatigue and failure over time, compatibility and long-term stability among diverse materials still represent major limitations to the widespread of FHE in commercial products.

Kirigami, the antique Japanese art of paper cutting, has been shown to be a simple and easy to implement technique to improve the flexibility of electronic devices, without affecting their intrinsic characteristics [39–41]. Some recent works employ the advantages of Kirigami patterning combined with printed devices to enhance device performances [42–44], thanks to its improved electro-mechanical stability with increased electrical conductivity stability over larger strain regimes [42]. This innovative method, paired with printed electronics, represents a promising solution for many applications of capacitive sensing [45].

However, Kirigami electrodes are not easy to incorporate in traditional sensors due to their important flexibility, which results in greater difficulty of integration to create a durable and robust connection while preserving the electrode flexibility.

In this work, we present a new hybrid capacitive sensor design approach, which addresses the above-mentioned challenges and limitations of FHE, by including the whole printed circuit board (PCB),

Table 1. Examples of other research groups employing FHE to implement flexible capacitive sensors for biopotential monitoring, with relative sensor characteristics.

Research Group	Size (mm^2)	Electrode type	Coupled capacitance (pF)	Bandwidth (Hz)
Ueno *et al* [34]	1000−7000	Textile	39−59	0.05−100
Rachim *et al* [35]	900	Hybrid textile	20	0.04−40
Gao *et al* [36]	400	Metal sputter deposition on plastic	7 − 35	0.3−100
Roland *et al* [7]	248−314	Various	77 − 733	60−1064
Lessard-Trembley *et al* [16]	853	Hybrid printed	51−107	0.475−210
Takano *et al* [37]	2000	Textile	57	0.5−100
Ng *et al* [38]	125	Hybrid printed	127	0.01−312

and not just single components, on the flexible device. Conceived as a novel method applicable to any printed capacitive sensor, the present work aims to improve the flexibility of FHE printed devices: the design method introduces an additional Kirigami printed layer to connect the rigid sensor PCB to the flexible Kirigami electrode, without affecting the mechanical and electrical characteristics of both sides. Achieving enhanced flexibility has the purpose of improving the robustness of the sensor to common MAs, such as the change in coupled surface area and variation in pressure between the sensor and the target body, producing a more stable and uniform signal acquisition.

To test the efficacy of the new design method, a sensor prototype was built, which comprises a traditional analog front-end (AFE) and a multi-layer printed Kirigami electrode, exhibiting remarkable flexibility and conformability on the electrode side while maintaining the robustness and reliability of conventional electronic components on the sensor side.

Compared to other FHE solutions found in literature [46–48], the novel sensor hybrid structure provides a new design approach that is effective, easy to implement and compatible with conventional manufacturing methods and materials, in order to produce a robust flexible capacitive electrode that can easily adapt to any curved surface, optimizing the sensing acquisition on the electrode-side, while being adaptable and compatible with conventional technologies and materials.

2. Materials and methods

The presented sensor structure includes three main functional layers: (1) the printed Kirigami electrode layer, composed of a single side capacitive electrode; (2) the printed Kirigami connecting structure, necessary to connect the flexible Kirigami layer to the PCB; (3) the sensor AFE, mounted on a rigid PCB.

2.1. Kirigami electrode and connecting layers

Kirigami technique was applied to both the electrode and connecting layers, representing the flexible side of the hybrid sensor. Their fabrication comprises two separate phases: the printing phase, to deposit the silver and insulating functional layers on a flexible dielectric substrate, and the cutting phase, to create the two different Kirigami structures by means of laser cutting.

2.1.1. Printing phase:

Both the electrode layer and the connecting layer are based on inkjet printed silver on a flexible dielectric substrate: in the case of the electrode layer, the printed silver electrode corresponds to the actual capacitive electrode, while the substrate acts as dielectric layer facing the sensing target; meanwhile, for the connecting layer, the printed silver area acts as a connecting base between the PCB and the flexible electrode, allowing to create a conductive path between the bottom of the PCB and the flexible electrode below.

Silver nano-particle ink from ANPPro (Silverjet P 40TE-20 C) was printed using a Ceradrop X-series printer loaded into a 13 pico-liter SAMBA cartridge. Kapton FPC 125 μm from American Durafilm was selected as dielectric substrate, and first cleaned with 99% acetone solvent. Four layers of the silver ink were printed in the form of $3 \times 3\,cm^2$ squares.

Intermittent drying steps using an Adphos near infrared drying lamp integrated into the Ceradrop system were performed to allow uniform drying of the printed ink. The printed structures were then sintered in a Mancorp MC301N reflow oven for 1 h at 300° in air. Dycotech DM-INI-7003 ink was chosen as insulating layer. Six layers of the insulating ink were inkjet printed atop the sintered silver electrodes, via Ceradrop printer, in the form of $4 \times 4\,cm^2$, with two central holes left empty to allow an electrical connection with the silver layer below. Each layer of the printed insulator ink was UV cured in place using the built ink UV cure lamp at $5.5\,mW\,cm^{-2}$ and $10\,mm\,s^{-1}$ conveyor velocity followed by a final cure step at 100% power and $1\,mm\,s^{-1}$ speed.

2.1.2. Laser cutting phase

The two layers were cut into two different Kirigami structures utilizing laser cutting (Samurai UV Marking System, DPSS Lasers, Inc.), with a final

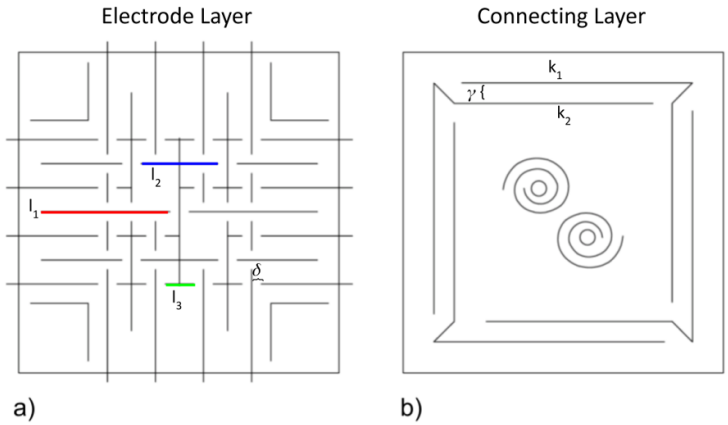

Figure 1. Laser-cut AutoCad design for the two different layers: (a) the Kirigami electrode pattern, where the sets of hierarchical cuts are represented by $l_1 = 20$ mm (in red), $l_2 = 12$ mm (in blue), $l_3 = 4.5$ mm (in green), and the hinges by $\delta = 1.5$ mm; (b) the closed-loop Kirigami connecting layer, with cuts of respectively $k_1 = 36$ mm and $k_2 = 29$ mm, distanced $\gamma = 3$ mm from each other.

dimension of $5 \times 5\,\text{cm}^2$, designed for the specific function of each layer (figure 1):

For the electrode layer, the chosen Kirigami pattern consists of standard squared, equally distanced, hierarchical perpendicular cuts, as shown in figure 1(a). The starting Kirigami design was taken from the structure realized in [45]: three different hierarchical levels of cuts were performed with a dimension of respectively $l_1 = 20$ mm, $l_2 = 12$ mm, $l_3 = 4.5$ mm, and hinges of width $\delta = 1.5$ mm. This type of structure allows for better conformability to any arbitrary non-flat surface, showing improved coupled capacitance compared to an equivalent, non-cut printed electrode [45, 49]. The flexibility and conformability of the electrode come from the subdivision of the printed layers into rotating square sub-units, with the connections between these units acting as free rotational hinges. This allows macroscopic deformation to occur mainly through rotation of the sub-units, rather than by attempting to deform the rigid sub-units themselves [39, 50]. Said mechanism allows the electrode to bend easily in all directions and adapt to any arbitrary non-flat surface, while maintaining intact its intrinsic characteristics. The design was slightly modified for the specific application: a portion of cuts on the central part was removed to leave enough non-cut surface available for the connection with the above connecting layer, and the external cuts were extended to reach the perimeter of the bigger electrode surface.

The connecting layer has the critical function of connecting the rigid PCB sensor to the flexible Kirigami structure of the electrode, without affecting its flexibility and while assuring a robust electrical and mechanical connection. The decision to employ a second, different, Kirigami structure as a middle layer represents a novel design approach to allow a robust but flexible connection between rigid components and flexible printed ones. For this reason, a closed-loop Kirigami structure, corresponding to the external cuts framing the printed pattern in figure 1(b), was chosen: external and internal cuts of respectively $k_1 = 36$ mm and $k_2 = 29$ mm, distanced $\gamma = 3$ mm from each other, enable a spring-like behavior in the connecting layer, allowing the central part to extend out-of-plane while remaining flat, in response to corners and borders bending or contracting [51].

The central silver printed part of the layer is conceived to be rigidly fixed to the PCB, while the external, cut frame is to be connected to the Kirigami electrode by its four angles exclusively. In this configuration, the Kirigami electrode is free to flex and conform to the target body, and at the same time, the central area where the PCB is attached remains flat even when the electrode below is flexed, because of the connecting layer structure that allows the motion of the central flat area out-of-plane, while the external frame bends to follow the electrode. The electrical connection between the two is assured by two central, silver-covered, spiral cuts. The spiral structure is not attached to the PCB, and is instead left free to move and elongate from the connecting layer to be linked to the central holes of the electrode layer, assuring a good electrical connection while maintaining the necessary flexibility. The contact is formed through silver epoxy paste (LOCTITE ABLESTIK 965-1 L) applied manually on top of the cut-through spiral connectors, and thermally cured at 100°C for 3 h. There are two points of contact built between the different layers: between the spirals and the prearranged dielectric holes on the electrode, and between the silver print of the connecting layer and the copper base of the PCB (figure 2).

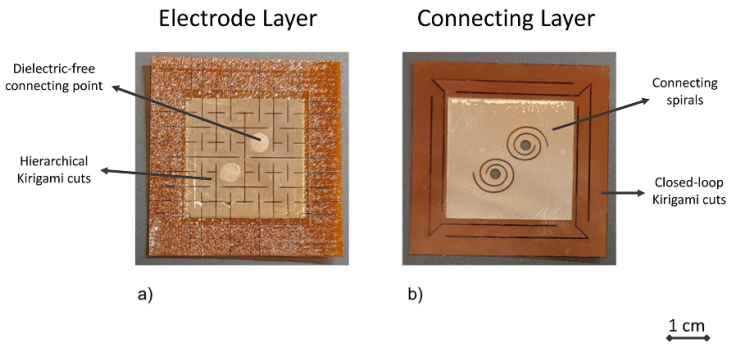

Figure 2. Printed layers after laser cut: (a) the Kirigami electrode layer (Kapton substrate and printed silver electrode covered by six layers of insulating ink, two circles of silver were left uncovered to allow for electrical connection with the connecting layer); (b) the closed-loop Kirigami connecting layer (Kapton substrate and printed silver, two holes surrounded by spirals were cut through, to allow for electrical end mechanical connection with the electrode layer).

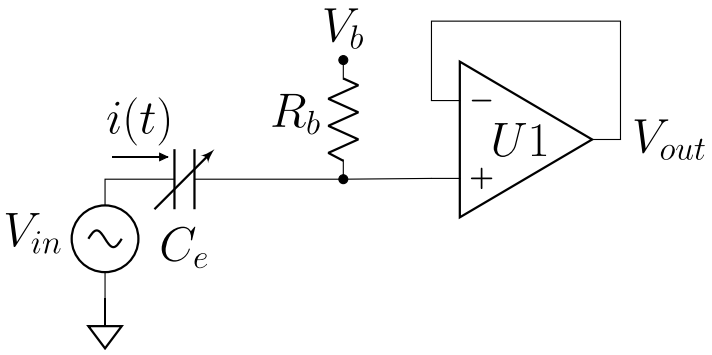

Figure 3. Simplified electrical model of analog front-end: V_{in} is the signal acquired by the electrode, C_e is the coupled capacitance between the sensor electrode and the second plate, V_b and R_b are the bias voltage and resistor, $U1$ is the op-amp connected in a buffer configuration and V_{out} the resulting acquired signal.

2.2. Analog front-end (AFE)

The AFE used in this work is a simple pre-amplifier circuit that allows the measurements of biological signals by capacitive sensing [52], consisting of an op-amp in a buffer configuration and a bias resistor, as schematically represented in figure 3.

The components are mounted on a rigid PCB of the size of $34.3 \times 34.3\,\text{mm}^2$, with an exposed copper bottom to allow the connection of the electrode to the input of the op-amp. The final multilayer structure and prototype sensor are illustrated in figure 4.

2.3. Experimental set up

To quantify the improvement in electrode performance between our novel Kirigami hybrid electrode and an arbitrary rigid electrode, a series of capacitive and electrical measurements were performed in different conditions of applied weights and second plate dimensions. For direct comparison with a rigid sensor, the same PCB was used as AFE, and a printed, single-layer electrode was rigidly glued to its bottom side, made of the same materials and with the same geometrical features of the equivalent Kirigami electrode, but with no Kirigami structure applied.

The goal of the performed tests is to provide an attentive but general characterization focused on specific electrical characteristics that are common to all types of electrical biosignals and are indicators of the effect of MAs on the acquisition process.

The capacitive measurements are performed using an impedance analyzer (Keysight E4990A), considering the electrode and the target body as two plates of a capacitor: the device, acting as the first plate, was positioned on a conforming insulating polyester sponge sample holder, with the dielectric layer facing up, and a conductive aluminum hemispherical body of varying diameter was placed on top of it to act as the second, non-planar plate of the capacitor (simulating different parts of the human body). The series capacitance between the aluminum plate and the Kirigami electrode connected to the sensor was measured on a frequency range of 20 Hz–1 kHz, to assure the consistency of the measurement: as the measurements revealed to be constant in this range, the capacitance acquired at 500 Hz was arbitrarily chosen as representative value. The main goal of these types of measurements is to verify that the multi-layer design is effective in allowing the Kirigami

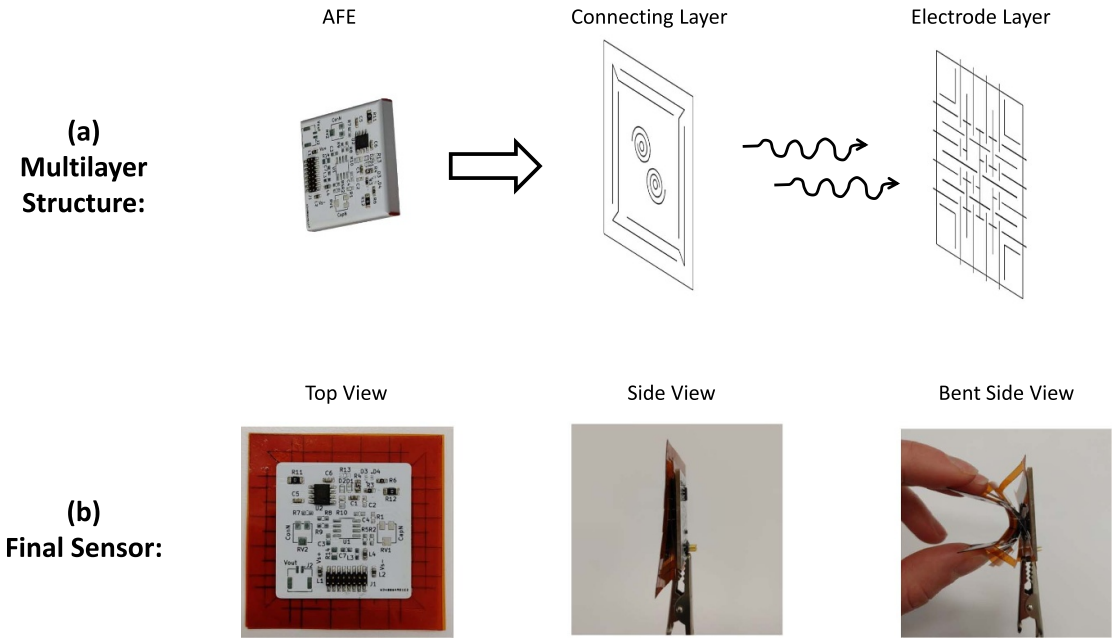

Figure 4. (a) Multilayer structure: the four corners of the Kirigami electrode and Kirigmi connecting layers are glued together to allow a mechanical connection without affecting the Kirigami electrode structure; at the same time the central point of the two spirals at the center of the connecting layer are electrically connected to the center of the electrode layer by conductive paste; on the other side, the AFE is pasted on the silver, non-cut side of the connecting layer by conductive paste, ensuring both good electrical and mechanical connection with the flexible layers, without limiting the respective flexibility. (b) Final sensor structure: top view of rigid circuit board connected, on the bottom, to the two flexible printed Kirigami layers; side view of the sensor in its relaxed state; side view of the sensor when the electrode layer is bent.

electrode to maintain its flexibility, thus showing good capacitive coupling with the sensing target, while being integrated on the rigid PCB.

The electrical measurements consist in the transmission of a sinusoidal signal from an arbitrary aluminum second plate to the sensor, imitating the signal acquisition of a biopotential coming from the body. The measurement set-up is the same as for the capacitive measurements, but in place of an Impedance Analyzer, a 1 Hz sinusoidal signal (Agilent 33 500B–Waveform Generator) was injected into the aluminum second plate, and the output pin of the sensor was connected to an oscilloscope (Keysight InfiniiVision DSOX3014T) in order to analyze the signal acquisition (figure 5(a)).

The measurement results consider two main signal characteristics: the amplitude and the cutoff frequency. The amplitude of the transmitted signal is considered as a reference point to obtaining satisfactory SNR in any actual sensing application, while the cut-off frequency represents an indication of the quantity of information transmitted, and thus, the quality of acquired signal.

The aluminum second plates considered in the experiments are one flat surface plate and different hemispheres of respectively 15 cm, 6.3 cm, 5.5 cm and 4.5 cm of diameter, corresponding to a curvature of 0, 0.13, 0.32, 0.36 and 0.44 cm^{-1}, respectively (figure 5(c)). The measurements are repeated for both the non-Kirigami and the Kirigami hybrid electrodes. Overloads of ≈1.1 kgf (2.5 lbf), ≈2.2 kgf (5 lbf) and ≈3.3 kgf (7.5 lbf) were applied to both cases, to test the uniformity of the electrode under different pressure applied. Each measurement (capacitive and electrical) was repeated 10 times, and the average value was considered. Lastly, the device was subjected to a 100 cycles bending test, at 60 degrees of bend, to evaluate the mechanical reliability of the structure. After that, the electrical measurements were repeated and the results compared with the first measured values.

3. Results

3.1. Capacitive measurements

In table 2 the average capacitance values measured for both the rigid sensor and the Kirigami hybrid sensor are listed, for different second plate curvatures. The measurements are the average of 6 measurement repetitions, with an applied weight of 2.2 kgf for each second plate.

In general, the trend for both sensors shows a decrease in value for increasing curvature. This is associated with the significant difference in second plate dimensions, which were specifically chosen to represent the behavior of the sensor in diverse situations (from flat to extremely curved). However, for all second plates considered the hybrid Kirigami sensor exhibits higher capacitance compared to the equivalent non-Kirigami one. Even in the extreme case of curvature 0.44 cm^{-1}, while still partly losing conformability due to the small dimension of the second plate, and thus significantly decreasing

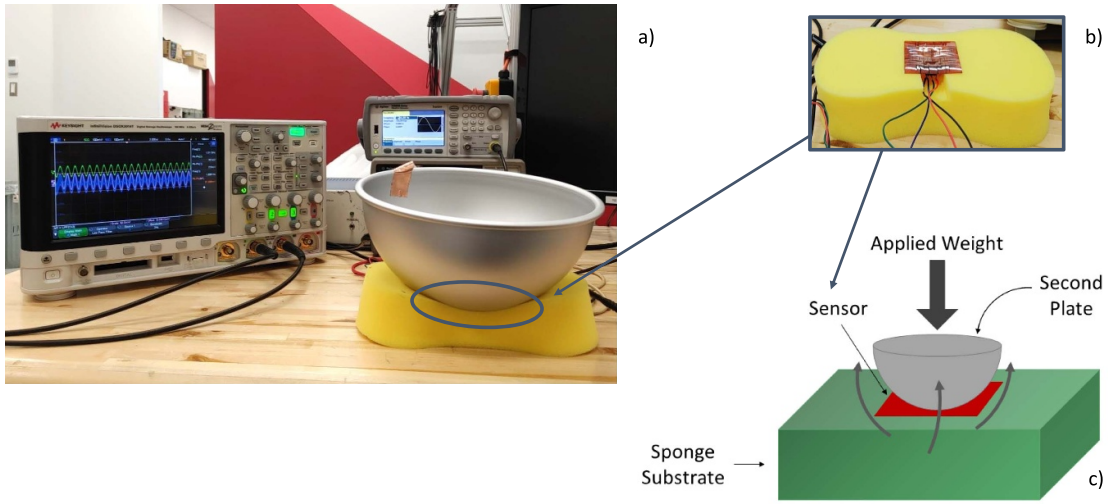

Figure 5. Electrical measurements setup: (a) second plate placed on top of the sensor, a single frequency (1 Hz) signal from the signal generator is injected into the second plate, acquired by the sensor and analyzed on the oscilloscope; (b) position of the sensor on the sponge holder, with the Kirigami electrode showing on top, before the application of the second body on it; (c) schematic representation of sensor and second plate setup during the measurements.

Table 2. Average measured coupled capacitance of both the Kirigami sensor and the equivalent rigid sensor, when applied to second plates of different curvatures.

	Average measured capacitance (pF)	
Second plate curvature (cm^{-1})	Rigid sensor	Kirigami sensor
0	70.69 ± 0.62	115.53 ± 0.69
0.13	69.96 ± 1.46	79.98 ± 2.08
0.32	37.63 ± 1.45	60.75 ± 3.87
0.36	29.23 ± 2.67	35.8 ± 3.34
0.44	25.97 ± 5.25	31.82 ± 3.77

in capacitive value, the recorded coupled capacitance presents an increase of $+32\%$ compared to its rigid counterpart.

The capacitive measurements of the single Kirigami hybrid sensor have been repeated, this time with different weights applied on top, and the results are represented in figure 6. Each value corresponding to the same second plate dimension exhibits negligible difference ($\leqslant 8\%$), indicating a good resistance of the Kirigami electrode to variations in applied pressure.

3.2. Electrical measurements

To validate the above results, the capacitive measurements were followed by electrical measurements of a sinusoidal 1 Hz signal transmitted from aluminum second plates of varied curvatures to the sensor, with different weights applied.

In figure 7, the acquired signal amplitudes, for different second plate diameters are represented. The different colors correspond to the different weights applied on top of the second plate. Consistently with the capacitive measurements, the amplitude trend inversely follows the curvature of the plates, confirming the importance of good conformability for better signal quality: measurements corresponding to a flat second plate exhibit a comparable signal amplitude for all weights applied; meanwhile, for increasing curvature a decrease in amplitude is recorded, as the capacitive coupling between the two sides deteriorates.

However, for a flexible Kirigami sensor, the difference in acquired signal amplitude, while still decreasing for bigger curvatures, shows a significant improvement (up to $+82\%$ for the bigger curvatures) compared to the non-Kirigami one.

In addition, the Kirigami sensor exhibits little to no variation when varying applied pressure, coherently with the results obtained in the capacitive measurements above.

The cutoff frequency of the sensor bandwidth was also measured, for the different curvatures and different weights applied. The cutoff frequency ($f_c = \frac{1}{2\pi RC}$) is by standard definition the frequency corresponding to an amplitude fall of 3 dB. Starting from the measured amplitude in figure 7, for each case the frequency of the transmitted signal was gradually decreased from 1 Hz, till the acquired signal amplitude decreased of 3 dB. The frequency registered on the oscilloscope corresponding to said amplitude was recorded as the resulting cutoff frequency.

In figure 8 the cutoff frequency variations for the different curvatures considered are plotted, divided by applied weight. For all cases, the f_c tends to grow for increasing curvature, however, for the non-flexible case the increase is significantly higher than the Kirigami case: in the case of the rigid electrode,

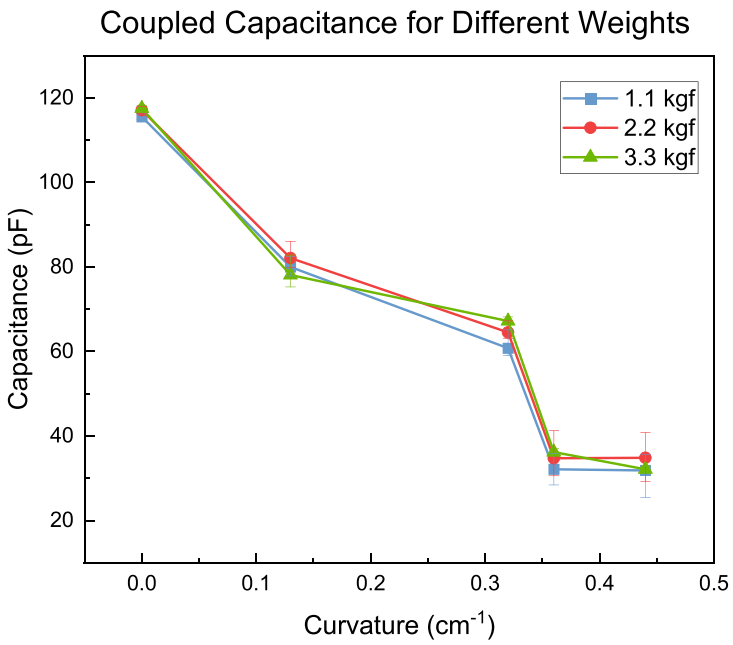

Figure 6. Measured coupled capacitance, for different second plate curvature, of Kirigami flexible sensor with weights of 1.1, 2.2 and 3.3 kgf applied on top of each second plate.

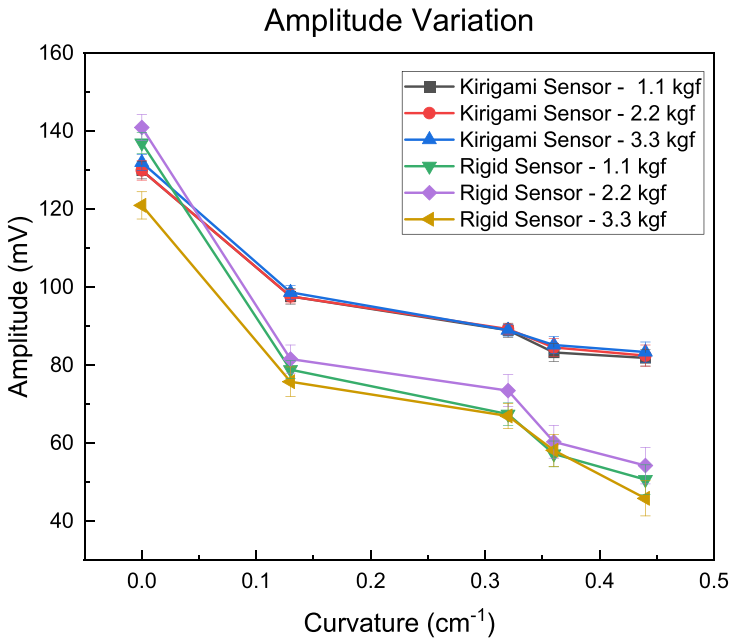

Figure 7. Measured amplitude variations of the acquired signal, for different second plate curvatures and different weights applied, comparing the performance of the Kirigami flexible sensor against the rigid sensor.

the gap in measured cutoff frequency for the zero curvature (flat second plate) to the 0.44 cm^{-1} hemisphere case is of +738 %; meanwhile, in case of the Kirigami electrode, the total increase for the smallest second plate is significantly smaller: +180 %. In addition, the different applied weights do not significantly affect the resulting f_c, showing good bandwidth uniformity for pressure variations during the measurements.

Finally, the sensor prototype was subjected to a mechanical reliability bending test, to monitor the effect of repetitive stress on the structure. The sensor was placed on a bending test machine and 100 bending cycles were executed at 60 degrees of bending (figure 9(b)). Following these cycles, the signal amplitudes were recorded once again, for the different diameters, at 1.1 kgf applied, and the results were compared to the previous measurements in figure 9(a).

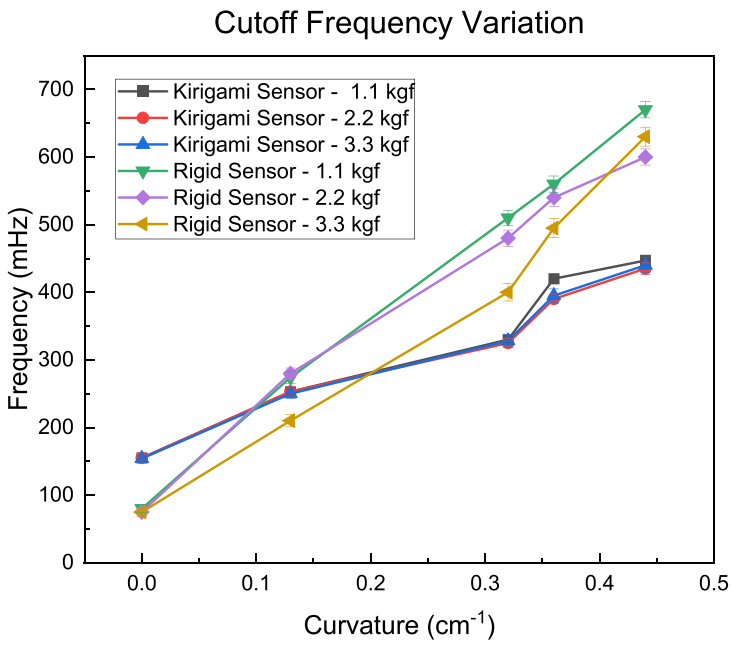

Figure 8. Measured cutoff frequency variations of the acquired signal, for different second plate curvatures and different weights applied, comparing the performance of the Kirigami flexible sensor against the rigid sensor.

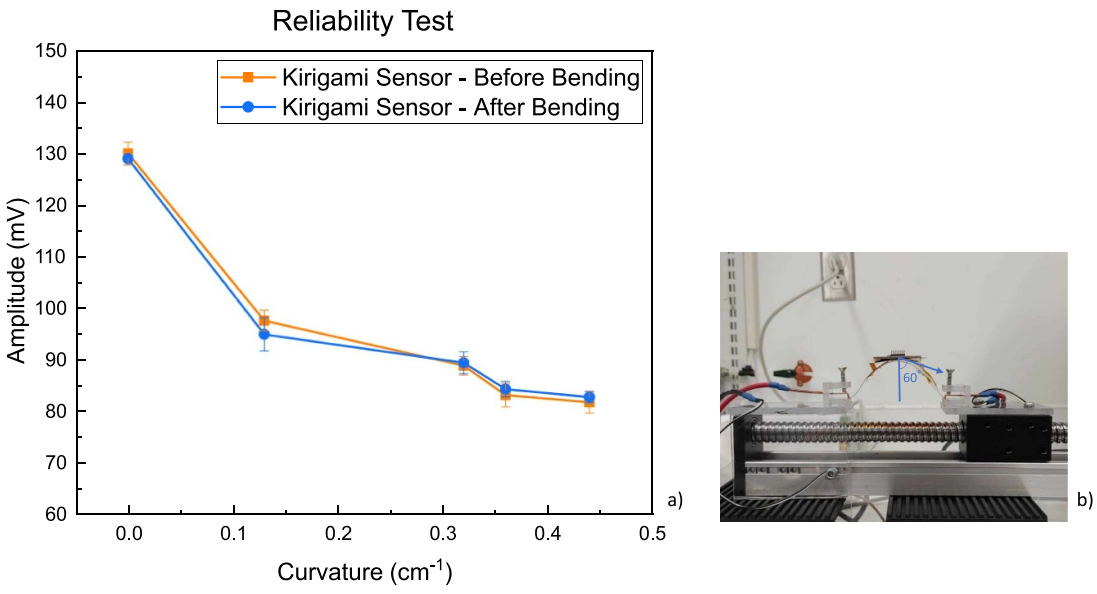

Figure 9. (a) Measured amplitude variations of the acquired signal, before and after 100 bending cycles, for different second plate curvatures at 1.1 kgf applied; (b) mechanical bending test setup: 100 bending cycles at 60 degrees of bend.

4. Discussion

The designed multi-layer Kirigami hybrid structure proved to be effective in allowing good flexibility and conformability of the electrode, while maintaining excellent electrical and mechanical contact throughout numerous bending and flexing tests while subjected to different weights.

The results of both the capacitive measurements and the sensor electrical measurements show consistency, indicating a direct relationship between the improved conformability brought by the novel Kirigami design and the performance of the sensor.

To better understand the effects of the electrode structure on the sensor it is useful to analyze each different aspect at time. First, as shown in both the capacitive measurements (table 2) and electrical recording (figure 7), the Kirigami structure allows for a better conformability to any arbitrary non-flat surface, leading to more surface of the electrode to establish a capacitive coupling with the target surface. As a consequence, the total capacitance established by the

sensor will increase, increasing the amplitude of the acquired signal and helping achieve a higher SNR.

If we consider that, for biopotential monitoring, a sensor is never used singularly but is usually part of an array of sensors that could be applied to different parts of the body, the remarkable flexibility of the Kirigami electrode favours the coupling of the different sensors of a system with the body, improving not only the performance of the single electrode but also the uniformity of the measurements for the whole system.

Moreover, a low cut-off frequency value is also extremely important for lossless signal acquisition: in the case of biosignals, many of them present a bandwidth in the very low frequency spectrum [9, 53]. The loss of information is not the only problem related to an inadequate cut-off frequency: while a slightly higher cut-off, with the right filtering, usually results in a still legible and satisfactory signal output, it can also introduce artifacts in the recordings that may lead to erroneous signal interpretation [16, 18, 54]. Being able to achieve a low cut-off frequency at the point of signal acquisition is thus important to ensure no information loss and/or no added artifacts, regardless of the sensing application. As shown in figure 8, the Kirigami sensor shows a lower cutoff value compared to the rigid sensor for all curved second plates considered, even the smaller ones.

Higher conformability of the single sensor allows us to achieve higher SNR, lower cutoff frequency and improved uniformity of the acquired signal, all before the filtering and post-processing phase.

In addition, the Kirigami multi-layer structure allows the electrode layer to be partially detached from the rigid PCB and free to bend and stretch when in contact with the body, while still maintaining good electrical contact. This added level of freedom favors the flexibility of the Kirigami electrode, allowing it to easily follow the curvature of the target body even with different pressures applied. As noticeable from figures 7 and 8, when varying the weight from 1.1 kgf to 2.2 kgf and 3.3 kgf, for each second plate considered, the measured values vary minimally, confirming the good adaptability of the sensor to pressure variations. Other works show examples of how increasing the pressure on the electrode serves to improve the capacitive coupling and, consequently, the sensor performance [55, 56]. Being susceptible to pressure changes, however, also makes the sensor more vulnerable to some type of MAs caused, for example, by the breathing pattern of the body or any partial movement that translates into a change of pressure on the electrode.

Finally, comparing amplitude measurements before and after the reliability bending test shows no significant difference. The multilayer Kirigami structure proves to be effective in minimizing the stress applied during bending, both on the electrode side, where the cuts critically reduce the effect of the stress on the printed conductive surface [45], and on the connections between electrode and AFE, where the middle Kirigami layer secures robust contact within the two while allowing freedom of movement, even after 100 bending cycles.

The Kirigami sensor presents improved conformability and flexibility, thanks to its novel designed multi-layer hybrid structure, allowing the electrode to conform well and maintain constant contact with the body under different pressures. This results in improved SNR and cut-off frequencies, without the need of additional signal post-processing.

5. Conclusions

In this work we presented a novel design and structure concept for printed electrodes for biopotential capacitive sensing based on Kirigami. The design comprises different layers cut in different Kirigami structures, each specifically designed for their individual function, allowing the electrode to be flexible and stretchable while being incorporated on traditional rigid PCBs and maintaining good electrical contact.

Capacitive and electrical measurements have been performed on the sensor under different conditions of weight applied and different sizes/shapes of sensing target in order to estimate their robustness to the most common MAs. The results obtained showed substantial improvement for the presented structure when compared to an analogous rigid sensor.

Both the flexibility of the Kirigami electrode and the compliance of the multi-layer hybrid structure lead to an improved conformability to any arbitrary second plate and increased robustness to variation of pressure, thus increasing the amplitude of the acquired signal, reducing the cutoff frequency and improving the uniformity of the measurements.

The novel design represents an easy-to-implement, robust, and effective method applicable to any printed capacitive sensors, allowing the integration of flexible printed electrodes on traditional rigid PCBs, improving the first's performance while maintaining the latter's reliability.

Data availability statement

All data that support the findings of this study are included within the article (and any supplementary files).

Author contributions

'Conceptualization, L Morelli.; methodology, L Morelli and A Wadhwa; validation, L Morelli; investigation, L Morelli; resources, L Morelli and A Wadhwa; writing–original draft preparation, L Morelli and A Wadhwa; writing–review and editing, L Morelli, R J Zednik and G Gagnon; supervision, R J Zednik, G Gagnon, S Cloutier and M Bolduc; project

administration, R J Zednik and G Gagnon; funding acquisition, R J Zednik and G Gagnon. All authors have read and agreed to the published version of the manuscript.'

ORCID iDs

Laura Morelli https://orcid.org/0000-0001-5627-5263
Arjun Wadhwa https://orcid.org/0000-0002-8026-5257
Sylvain Cloutier https://orcid.org/0000-0003-0092-5241
Martin Bolduc https://orcid.org/0009-0008-2758-7573
Ghyslain Gagnon https://orcid.org/0000-0001-9484-7218
Ricardo J Zednik https://orcid.org/0000-0002-2767-2961

References

[1] Bandodkar A J and Wang J 2014 *Trends Biotechnol.* **32** 363–71
[2] Santos C C D, Lucena G N, Pinto G C, Júnior M J and Marques R F 2021 *Med. Devices Sensors* **4** e10130
[3] Promphet N, Ummartyotin S, Ngeontae W, Puthongkham P and Rodthongkum N 2021 *Analytica Chim. Acta* **1179** 338643
[4] Yun S M, Kim M H, Kwon Y W, Kim H B, Kim M J, Park Y G and Park J U 2021 *Appl. Sci.* **11** 1235
[5] Uguz D U, Dettori R, Napp A, Walter M, Marx N, Leonhardt S and Antink C H 2020 *Sensors* **20** 6288
[6] Baek H, Lee H, Lim Y and Park K 2013 *Biomed. Eng. Lett.* **3** 158–69
[7] Roland T, Wimberger K, Amsuess S, Russold M F and Baumgartner W 2019 *Sensors* **19** 961
[8] Lee J S, Heo J, Lee W K, Lim Y G, Kim Y H and Park K S 2014 *Sensors* **14** 14732–43
[9] Kaniusas E 2019 *Biomedical Signals and Sensors III: Linking Electric Biosignals and Biomedical Sensors* (Springer)
[10] Lim Y G, Kim K K and Park K S 2007 *IEEE Trans. Biomed. Eng.* **54** 718–25
[11] Lim Y G, Lee J S, Lee S M, Lee H J and Park K S 2014 *Ann. Biomed. Eng.* **42** 2218–27
[12] Taji B, Shirmohammadi S, Groza V and Batkin I 2014 *IEEE Trans. Instrum. Meas.* **63** 1412–22
[13] Venkatachalam K L, Herbrandson J E and Asirvatham S J 2011 *Circ. Arrhythmia Electrophysiol.* **4** 965–73
[14] Chatterjee S, Thakur R S, Yadav R N, Gupta L and Raghuvanshi D K 2020 *IET Signal Process.* **14** 569–90
[15] Sirtoli V G, Liamini M, Lins L T, Lessard-Tremblay M, Cowan G, Zednik R J and Gagnon G 2023 *IEEE Trans. Biomed. Circuits Sys.* **17** 394–412
[16] Lessard-Tremblay M, Weeks J, Morelli L, Cowan G, Gagnon G and Zednik R J 2020 *Sensors* **18** 5156
[17] Wang T W, Zhang H and Lin S F 2020 *IEEE Sens. J.* **20** 9265–73
[18] Berson A S and Pipberger H V 1966 *Am. Heart J.* **71** 779–89
[19] Xiao Z, Xing Y, Yang C, Li J and Liu C 2022 *IEEE Instrum. Meas. Mag.* **25** 53–61
[20] Khan Y, Thielens A, Muin S, Ting J, Baumbauer C and Arias A C 2020 *Adv. Mater. Special Issue: Flexible Hybrid Electron.* **32** 1905279
[21] Wiklund J, Karakoc A, Palko T, Yiğitler H, Ruttik K, Jäntti R and Paltakari J 2021 *J. Manuf. Mater. Process.* **5** 89
[22] Kim H S, Kang J S, Park J S, Hahn H T, Jung H C and Joung J W 2009 *Compos. Sci. Technol.* **69** 1880–6
[23] Beedasy V and Smith P J 2020 *Materials* **13** 704
[24] Nayak L, Mohanty S, Nayaka S K and Ramadoss A 2019 *J. Mater. Chem.* **7** 8771–95
[25] Lee S M, Sim K S, Kim K K, Lim Y G and Park K S 2010 *Med. Biol. Eng. Comput.* **48** 447–57
[26] Baek H J, Li H J, Lim Y G and Park K S 2012 *IEEE Trans. Biomed. Eng.* **59** 3422–31
[27] Dong R, Liu X, Cheng S, Tang L, Chen M, Zhong L, Chen Z, Liu S and Jiang X 2020 *Adv. Healthcare Mater.* **32** 1902333
[28] Taccola S, Poliziani A, Santonocito D, Mondini A, Denk C, Ide A N, Oberparleiter M, Greco F and Mattoli V 2021 *Sensors* **21** 1197
[29] Cai J, Cizek K, Long B, McAferty K, Campbell C G, Allee D R, Vogt B D, Belle J L and Wang J 2009 *Sensors Actuators* B **137** 379–85
[30] Ohring M 2002 *Materials Science of Thin Films: Deposition and Structure* 2nd edn (Academic)
[31] Hao W, YongAn H and ZhouPing Y 2022 *Sci. china Technol. Sci.* **65** 1995–2006
[32] Tuncel Y, Bhat G and Ogras U Y 2020 *2020 IEEE 38th VLSI Test Symp. (VTS)*
[33] Yan J, Chen A and Liu S 2024 *Alexandria Eng. J.* **86** 405–14
[34] Ueno A, Akabane Y, Kato T, Hoshino H, Kataoka S and Ishiyama Y 2007 *IEEE Trans. Biomed. Eng.* **54** 759–66
[35] Rachim V P and Chung W Y 2016 *IEEE Trans. Biomed. Circuits Syst.* **10** 1112–8
[36] Gao Y, Soman V V, Lombardi J P, Rajbhandari P P, Dhakal T P, Wilson D G, Poliks M D, Ghose K, Turner J N and Jin Z 2020 *IEEE Trans. Instrum. Meas.* **69** 4314–23
[37] Takano A, Ishigami H and Ueno A 2021 *Sensors* **21** 812
[38] Ng C L, Reaz M B I, Crespo M L, Cicuttin A, Bin Shapiai M I, Bin Md Ali S H, Binti Kamal N and Chowdhury M E H 2023 *IEEE Trans. Instrum. Meas.* **72** 4007213
[39] Zhai Z, Wu L and Jiang H 2021 *Appl. Phys. Rev.* **8** 041319
[40] Choi G P T, Dudte L H and Mahadevan L 2019 *Nat. Mater.* **18** 999–1004
[41] Yang S, Choi I and Kamien R D 2016 *MRS Bull.* **41** 130–8
[42] Li B M, Kim I, Zhou Y, Mills A C, Flewwellin T J and Jur J S 2019 *Adv. Mater. Technol.* **4** 673–83
[43] Yu H C, Hao X P, Zhang C W, Zheng S Y, Du M, Liang S, Wu Z L and Zheng Q 2021 *Small* **17** 2103836
[44] Zhang S, Wang S, Zheng Y, Yang R, Dong E, Lu L, Xuan S and Gong X 2021 *Compos. Sci. Technol.* **7** 216
[45] Morelli L, Gagnon G and Zednik R J 2023 *IEEE J. Flexible Electron.* **2** 472–80
[46] Kim Y, Mahmood M, Lee Y, Kim N, Kwon S, Herbert R, Kim D, Cho H and Yeo W 2019 *Adv. Sci.* **6** 1900939
[47] Poliks M, Turner J, Ghose K, Jin Z, Garg M, Gui Q, Arias A, Kahn Y, Schadt M and Egitto F 2016 *2016 IEEE 66th Electronic Components and Technology Conf. (ECTC)* pp 1623–31
[48] Liu S, Shah D and Kramer-Bottiglio R 2021 *Nat. Mater.* **20** 851–8
[49] An N, Domel A G, Zhou J, Rafsanjani A and Bertoldi K 2019 *Adv. Funct. Mater.* **30** 1906711
[50] Grima J N and Evans K E 2000 *J. Mater. Sci. Lett.* **19** 1563–5
[51] Tao J H, Khosravi V D and Li S 2022 *Adv. Sci.* **3** 9217–23
[52] Sun Y and Yu X B 2016 *IEEE Sens. J.* **16** 2832–53
[53] Bronzino J D 2006 *Medical Devices and Systems* 3rd edn (*The Biomedical Engineering Handbook*) (Taylor & Francis)
[54] Driel J V, Olivers C N L and Fahrenfort J 2021 *J. Neurosci. Methods* **352** 109080
[55] Ng C L and Reaz M B I 2019 *Measurement* **145** 460–71
[56] Kim S, Lee S and Jeong W 2020 *Polymers* **12** 2406